Received: 18 April 2020 | Revised: 6 August 2020 | Accepted: 8 August 2020

DOI: 10.1111/jace.17422

ORIGINAL ARTICLE

Journal of the American Ceramic Society

The effect of cesium content on the thermodynamic stability and chemical durability of $(Ba,Cs)_{1.33}(Al,Ti)_8O_{16}$ hollandite

Mingyang Zhao[1] | **Jake W. Amoroso**[2] | **Kalee M. Fenker**[2] | **David P. DiPrete**[2] | **Scott Misture**[3] | **Stephen Utlak**[4] | **Theodore Besmann**[4] | **Kyle Brinkman**[1]

[1]Department of Materials Science and Engineering, Clemson University, Clemson, SC, USA

[2]Savannah River National Laboratory, Aiken, SC, USA

[3]Kazuo Inamori School of Engineering, Alfred University, Alfred, NY, USA

[4]Nuclear Engineering Program, Department of Mechanical Engineering, University of South Carolina, Columbia, SC, USA

Correspondence
Kyle Brinkman, Department of Materials Science and Engineering, Clemson University, Clemson, SC 29634, USA.
Email: ksbrink@clemson.edu

Present address
Stephen Utlak, Materials Science and Technology Division, Oak Ridge National Laboratory, Oak Ridge, TN, USA

Funding information
Center for Hierarchical Waste Form Materials, an Energy Frontier Research Center funded by the U.S. Department of Energy, Office of Science, Basic Energy Sciences, Grant/Award Number: DE-SC0016574

Abstract

Titanate-based hollandite ceramics are promising nuclear waste forms for Cs immobilization. In this work, a series of Al-substituted hollandite $(Ba,Cs)_{1.33}(Al,Ti)_8O_{16}$ was investigated across a broad compositional range with varying Cs content. Powder X-ray diffraction showed that all samples exhibited a tetragonal hollandite phase. Enthalpies of formation determined by high-temperature melt solution calorimetry indicated enhanced thermodynamic stability with increased Cs content, which generally agreed with sublattice-based thermodynamic calculations. Moreover, enthalpies of formation of the samples were primarily affected by three factors: (a) relative sizes of cations on the A-sites and B-sites, (b) tolerance factor, and (c) optical basicity. Fractional element release revealed that Cs retention was significantly improved for the high Cs-containing hollandite compositions, which were supported by the evolution of microstructure of the pre and postleach particles. Elution studies of Al-substituted hollandite spiked with radioactive ^{137}Cs indicated that transmutation of Cs to Ba in the hollandite was accompanied by an increase in the retention of the Cs decay product, suggesting long-term stability of Al-substituted hollandite phase.

1 | INTRODUCTION

Nuclear power plants operating in many countries, including China, United States, France, and Japan provide efficient and emission-free electricity as compared to traditional fossil fuels. However, challenges remain concerning the re-processing and treatment of radioactive wastes from nuclear reactors in advanced nuclear fuel cycles. Cesium (Cs) is one radionuclide of concern for contemporary immobilization efforts due to its high toxicity and mobility in the environment which may impact the biosphere.[1,2]

Titanate-based hollandite has been considered as one of the most promising host matrices for Cs immobilization due to its structural[3] and thermodynamic stability[4-7] as well as its chemical durability.[8-10] These hollandites are described by the general formula $(Ba_x^{2+}Cs_y^{+})(M,Ti^{4+})_8O_{16}$ $(0 < x + y < 2)$, where M is a trivalent or divalent cation ($M = Al^{3+}$, Ga^{3+}, Fe^{3+}, Zn^{2+}, Mg^{2+}, etc).[4-7,11,12] In a unit cell, the hollandite structure consists of eight $(M,Ti)O_6$ octahedra which are linked by corners and edges to form tunnels. The positions in the tunnels occupied by Ba^{2+}/Cs^{+} are A sites, whereas the sites occupied by M/Ti^{4+} in the octahedra framework are B

sites. Al-substituted hollandite $(Ba_x^{2+}Cs_y^{+})(Al^{3+},Ti^{4+})_8O_{16}$ has previously been investigated, including synthesis,[13] crystallography,[9,14,15] durability,[8,16] thermochemistry,[4,5] and radiation resistance.[17,18] However, there remain significant questions concerning the impact of Cs stoichiometry on the thermodynamic stability and chemical durability. This work presents a systematic investigation of Al-substituted hollandite across a broad compositional range, which will benefit future design and optimization of waste forms.

A series of $Ba_{1.33-x}Cs_xAl_{2.66-x}Ti_{5.33+x}O_{16}$ $(0 \leq x \leq 1)$ with a broad compositional range of Cs content was successfully synthesized. High-temperature oxide melt solution calorimetry was utilized to determine the effect of Cs content on thermodynamic stability, whereas calculations based on a reoptimized sublattice model were used to verify experimental results. The principal factors that impact the thermodynamic stability are discussed along with performance-based leaching tests in order to investigate the effect of Cs content on chemical durability.

2 | EXPERIMENTAL PROCEDURE

2.1 | Sample synthesis

Five hollandite samples were studied: $Ba_{1.33}Al_{2.67}Ti_{5.33}O_{16}$ (H1), $Ba_{1.167}Cs_{0.166}Al_{2.50}Ti_{5.50}O_{16}$ (H2), $Ba_1Cs_{0.33}Al_{2.33}Ti_{5.67}O_{16}$ (H3), $Ba_{0.667}Cs_{0.667}Al_2Ti_6O_{16}$ (H4), and $Ba_{0.33}Cs_1Al_{1.67}Ti_{6.33}O_{16}$ (H5). Samples were synthesized via a solid-state reaction route for the majority of measurements. Samples with low Cs content were difficult to obtain without trace amounts of secondary phase and therefore select samples were synthesized via a solution combustion synthesis (SCS) route in order to complement the calorimetry measurements and to prepare samples spiked with radioactive ^{137}Cs for leaching studies.

2.1.1 | Solid-state synthesis

Stoichiometric amounts of reagent oxides and carbonates were added into a 100 mL polyethylene (PE) bottle with zirconia grinding media and deionized (DI) water to fill ≤ 80% by volume and mixed in a Turbula® mixer for approximately 20 minutes. The resultant slurry was rinsed from the milling media and dried overnight in laboratory oven at ≤ 90°C. For each composition, the dried material was transferred to a covered crucible (Pt 10%Rh) and heated to 1000°C from room temperature. After 1 hour, each crucible was removed from the furnace and air cooled. The material was ground in a ring-pulverizer (Angstrom), returned to the crucible, placed into a furnace preheated to 1000°C, and heated to 1200°C. After a 6 hours isothermal hold, the crucible was removed and air cooled. The grinding and reheating steps were then repeated with a 24 hours isothermal hold at 1200°C. The phase purity of the resulting material was confirmed by powder X-ray diffraction (XRD).

2.1.2 | Solution combustion synthesis

A solution combustion synthesis (SCS) method was developed to synthesize phase pure hollandite in small quantity with minimal Cs loss. Precursor metal nitrate solutions were mixed with appropriate ratios of urea and glycine based on the target stoichiometry and metal cation. Titanyl nitrate was prepared separately as meta-titanic acid from hydrolyzed and rinsed isopropoxide, to which nitric acid was added. The meta-stable titanyl nitrate solution was used within 2 hours of preparation. Urea, glycine, the metal nitrates (excluding Ti) were dissolved in a minimal volume of deionized water, generally 2-4 mL. Mild heating on a hot plate was used to facilitate complete dissolution. That solution was transferred to a 50 mL Erlenmeyer flask to which the titanyl nitrate was added. The resulting solution exhibited a yellow tinge and was swirled to encourage mixing. The flask was placed in a furnace and heated to 500°C at a rate of approximately 20°C/min. Typically, combustion occurred between 400°C and 500°C shortly after the water boil off. Following the combustion reaction, samples were heated to 900°C and immediately cooled upon reaching maximum temperature. This methodology, with only minor modifications, was also used to synthesize hollandite doped with ^{137}Cs. Specifically, a mixture of Cs/^{137}Cs nitrate, was added to the meta-titanic acid to form the titanyl nitrate. Additional nitric acid was added based on stoichiometric reaction calculations; generally, about 1 mL of nitric acid was needed for each reaction and yielded approximately 1 g of material. The ^{137}Cs was extracted with a resorcinol formaldehyde-based extraction from dissolved used nuclear fuel (UNF) being reprocessed in the Savannah River Site H-Canyon radiological separation facility. Three hollandite samples, referred to as H4, H4-plus, and H5, were prepared as compositions corresponding to their respective prefix. The phase purity of the resulting material was confirmed by XRD.

> Caution! ^{137}Cs is radioactive and emits a high-energy gamma emission through its decay processes. ^{137}Cs poses potential serious health risks and should be handled at properly licensed facilities with proper engineering controls.

2.2 | Characterization

Powder X-ray diffraction (XRD) measurements were conducted by Rigaku Ultima IV diffractometer with monochromatic CuK_α

TABLE 1 Target and analyzed compositions of the samples[a]

Sample	Target composition	Analyzed composition
H1	$Ba_{1.33}Al_{2.66}Ti_{5.34}O_{16}$	$Ba_{1.53}Al_{2.54}Ti_{5.34}O_{16}$
H2	$Ba_{1.167}Cs_{0.163}Al_{2.50}Ti_{5.50}O_{16}$	$Ba_{1.25}Cs_{0.16}Al_{2.44}Ti_{5.50}O_{16}$
H3	$Ba_1Cs_{0.33}Al_{2.33}Ti_{5.67}O_{16}$	$Ba_{1.02}Cs_{0.32}Al_{2.32}Ti_{5.67}O_{16}$
H4	$Ba_{0.667}Cs_{0.667}Al_2Ti_6O_{16}$	$Ba_{0.67}Cs_{0.72}Al_{1.98}Ti_6O_{16}$
H5	$Ba_{0.33}Cs_1Al_{1.67}Ti_{6.33}O_{16}$	$Ba_{0.34}Cs_{1.07}Al_{1.64}Ti_{6.63}O_{16}$

[a]Compositions were normalized to Ti and oxygen contents were corrected to achieve charge balance.

radiation (λ = 1.54 Å) to analyze the crystal structure of hollandite samples. The data were collected from 10° to 80° 2θ with a 0.02° step size. Microstructure of hollandite samples was investigated by a Hitachi SU6600 scanning electron microscopy (SEM) equipped with energy dispersive X-ray spectroscopy (EDS) analysis (Oxford). Chemical compositions of the hollandite samples were determined by energy dispersive X-ray spectroscopy (EDS) analysis and inductively coupled plasma-mass spectroscopy (ICP-MS). These analyzed compositions are given in Tables 1 and S1. Elemental concentrations in leaching solution were measured by ICP-MS and inductively coupled plasma-atomic emission spectroscopy (ICP-AES). Details about instrument and experimental procedure can be found by prior studies.[6,7,12]

2.3 | High-temperature oxide melt solution calorimetry

High-temperature oxide melt solution calorimetry was performed using an AlexSYS 1000 calorimeter operating at 702°C. In a drop solution calorimetry experiment, approximately 5-10 mg weighed samples were loosely pressed into pellets and dropped from room temperature into the molten sodium molybdate ($3Na_2O{\cdot}4MoO_3$) solvent in a platinum crucible in the calorimeter. The calorimeter assembly was flushed with dry air at ~60 mL/min, whereas dry air was bubbled through the solvent at ~7 mL/min to stir the melt and aid sample dissolution. Measurements were performed at least six times for each composition to acquire statistically reliable data. The calorimeter was calibrated utilizing the heat content of α-alumina (99.995%). This methodology has been well established and described previously.[19,20]

2.4 | Sublattice-based thermodynamic calculations

A series of thermodynamic functions to describe equilibrium behaviors of hollandites in a high-level radioactive waste system was developed by Utlak et al[21] Based upon that effort, a sublattice model was further developed using the compound energy formalism (CEF)[22-27] to represent the nonstoichiometry of hollandite compounds. Al^{3+} is the only dopant in this work, so a new four sublattice CEF hollandite model was defined as:

$$\left(Ba^{2+},Cs^{+},Va\right)_2\left[Ti^{4+},Al^{3+}\right]_4\left\{Ti^{4+}\right\}_4\left\langle O_{16}^{2-}\right\rangle,$$

where Va represents vacancies along tunnels. Detailed description of the sublattice model and its feasibility to derive Gibbs energies of hollandite solid solution can be found by Utlak et al.[21]

Although Utlak et al[21] reported enthalpies of formation of Al-substituted hollandite in their original work, it was necessary to incorporate the new enthalpic data generated in this work and accordingly adjust relevant model parameters to maintain good agreement between model calculations and experimental data. Consequently, the Gibbs energies of hollandite end members as well as Ba and Cs titanate end members were adjusted based on the new experimentally derived $\Delta H_{f,ox}$ values in Table 2, and the adjusted Gibbs energies were listed in Table S2. The adjustment of the reoptimized data was too small to affect the original calculated compositions,[21] so it was not reproduced here. In addition, all other model parameters used in the original study were retained in this work.[21]

2.5 | Chemical durability

2.5.1 | Aqueous leaching tests

As-synthesized hollandite samples were prepared for accelerated leaching measurements following the guidelines in ASTM C1285-14 product consistency test (PCT).[28] The synthesized powders were not amenable to grinding due to their friable nature. Therefore, the samples were not ground; instead a representative sample was collected as a sieve fraction (ie, −100/+200) to obtain an initially consistent particle size across all leaching tests. Sieved particles were washed in water and alcohol yielding enough material to perform duplicate testing with approximately 1 g of particles per test. Particles were added into ~10 mL of water in stainless steel vessels, sealed with threaded enclosures, and placed in an oven at 90°C for seven days. A reference material and two

blanks were run in parallel with the samples. Following the test duration, pH was measured, and the leachates were filtered and diluted with nitric acid in a ratio of 6 mL of acid to 4 mL of leachate. The leachates were stored refrigerated prior to elemental analysis. The fractional release rate of element *i* in the sample (FR_i) was calculated using Equation 1:

$$\mathrm{FR}_i = \frac{C_i V}{m_s f_i}, \tag{1}$$

where FR_i = fractional elemental release (unitless), C_i = concentration of element *i* in the leachate (g/L), V_s = leachate volume (L), m_s = sample mass (g), and f_i = fraction of element *i* in the unleached sample (unitless).

2.5.2 | Elution studies of ^{137}Cs-doped Al-substituted hollandite

Three samples of hollandite, referred to as H4, H4-plus, and H5, were tested and correspond to compositions H5 and H4, the latter of which was tested in duplicate. Hollandite samples were subjected to a deionized (DI) water leaching study measuring the leaching rates of the ^{137}Cs ($t_{1/2}$ = 30 y) bound in the hollandite versus the ^{137m}Ba daughter ($t_{1/2}$ = 2.552 m). ^{137m}Ba emits a 662 keV gamma ray when it decays to the ground state. As-synthesized hollandite was loaded into a 2 mL bed volume BIO-RAD Poly-Prep chromatography column mounted on a twelve-position vacuum box (Eichrom Technologies). Samples were washed between 10 and 20 times with DI water in 5 to 50 mL aliquots. Each aliquot was analyzed after contact with the hollandite for the characteristic 662 keV gamma ray using a lanthanum bromide (LaBr) gamma spectrometer with a 2″ × 2″ LaBr crystal. The LaBr gamma spectrometer was powered with a Mirion Industries digital multichannel analyzer (MCA). Subsequently, each aliquot was analyzed by gamma after ^{137}Cs and ^{137m}Ba had come into radiological equilibrium. Each aliquot was counted 30 times; twenty-five 10-second counts were made initially, followed by five 60-second counts. A subset of aliquots was analyzed by ICP-MS and XRD was performed on the materials after washing.

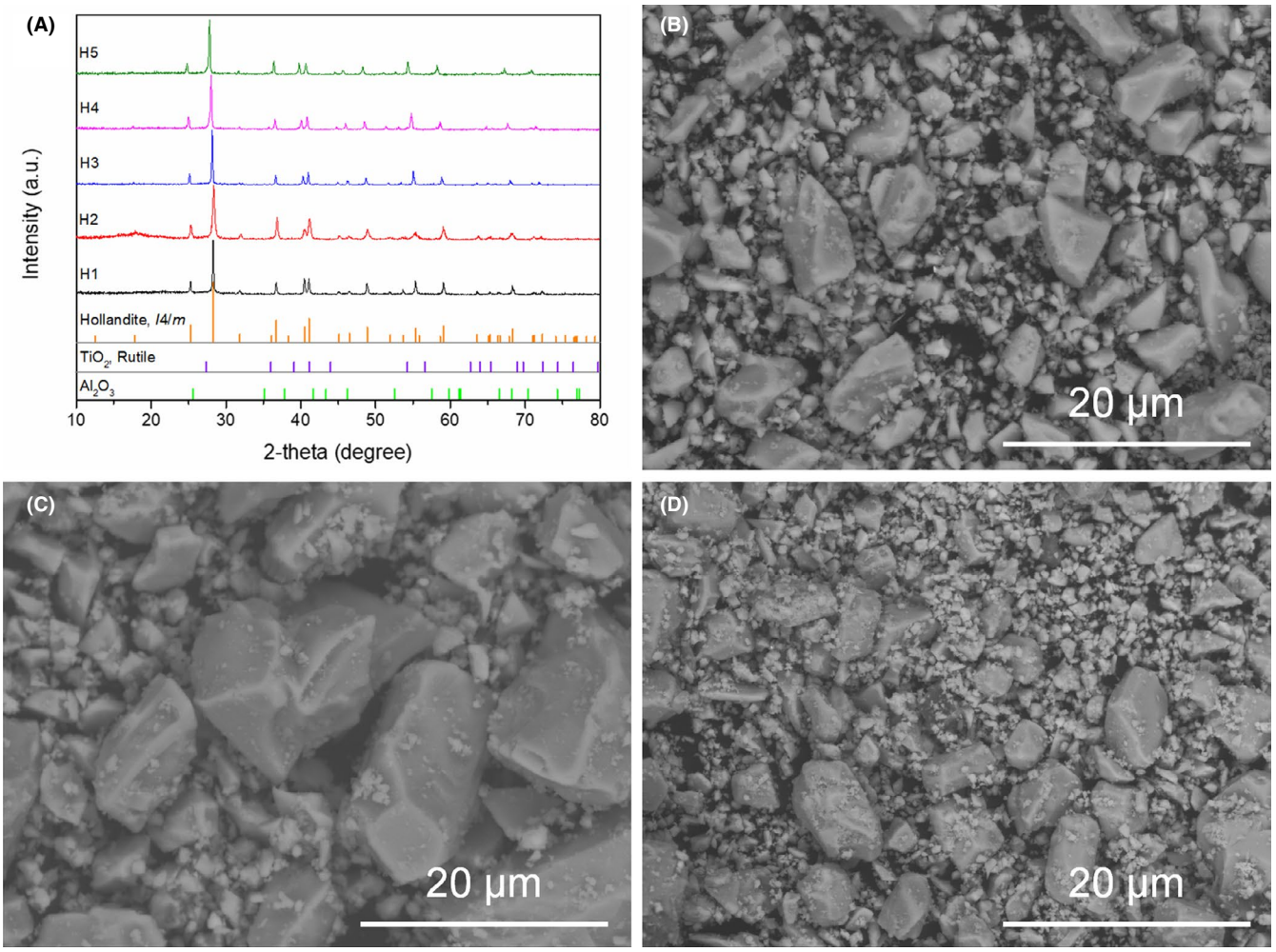

FIGURE 1 (A) XRD patterns of hollandite samples with varying Cs content; the microstructure and morphology of (B) H1, (C) H3, (D) H5 [Color figure can be viewed at wileyonlinelibrary.com]

3 | RESULTS AND DISCUSSION

3.1 | Characterization

XRD patterns of as-synthesized samples H1-H5 are displayed in Figure 1A using $Ba_{1.242}Al_{2.484}Ti_{5.516}O_{16}$ (PDF#78-0013, *I*/4*m*) as the reference. In Figure 1A, all samples exhibit tetragonal hollandite structure (space group: *I*4/*m*) across the wide range of Cs content, with a small amount of the secondary phases (eg, Al_2O_3 corundum and TiO_2 rutile) present. The actual chemical formula of the hollandite phase was given in Table 1. The amount of the secondary phases were reported in Table S1. These analyzed results were used to calculate enthalpies of formation. In order to investigate the effect of Cs content on the microstructure, as-synthesized samples without ball milling and grinding were used. As shown in Figure 1B-D, back-scattered electron (BSE) images of the select samples show that all samples exhibit microrods along with a few smaller chunks. Moreover, both length and width of those hollandite rods increases with increasing Cs content increases. This structural feature has been previously observed in Ga-substituted hollandite systems.[29]

3.2 | Thermodynamic stability

3.2.1 | Experimentally derived enthalpies of formation

Enthalpies of formation of hollandite samples were determined by high-temperature oxide melt solution calorimetry. The enthalpies of drop solution (ΔH_{ds}) of hollandite samples and α-Al_2O_3 (Inframat Advanced Materials, 99.995%) measured in the molten $3Na_2O{\cdot}4MoO_3$ solvent at 702°C are given in Tables 2 and 3, respectively. Using these values and previously reported ΔH_{ds} and the enthalpies of formation at 25°C from the elements ($\Delta H_{f,el}$) of BaO, Cs_2O and TiO_2 (in Table 3), the enthalpies of formation at 25°C from constituent oxides ($\Delta H_{f,ox}$) and $\Delta H_{f,el}$ were calculated using thermochemical cycles. Table 4 serves as an example to use thermochemical cycles to obtain $\Delta H_{f,ox}$ and $\Delta H_{f,el}$ values.[30-33] Analyzed compositions of the major hollandite phases and the minor secondary phases in Tables 1 and S1 were used to refine the enthalpies of formation. It is notable that as-synthesized samples were further ball milled and ground well by agate mortar and pestle to obtain fine and relatively homogeneous powder samples before dropping experiments to aid in dissolution. Although the postground powder has different-sized micrometer-scale particles, the effect of surface area and particle size on the enthalpy of formation is insignificant unless the particle size of the measured oxides is smaller than 100 nm.[34,35] Therefore, the impact of the particle-size effect is negligible in this work comparing to the relatively large experiment errors.

In Figure 2, the $\Delta H_{f,ox}$ values of all samples are exothermic, and are close to the previously reported $\Delta H_{f,ox}$ values of Al-substituted hollandite with different compositions,[4,5] indicating that they are thermodynamically stable relative to their binary constituent oxides. Moreover, the $\Delta H_{f,ox}$ value becomes more negative and thus more enthalpically stable as the Cs content increases, which generally agrees with the trend calculated by Wen et al[36] using density functional theory (DFT) methodology. In addition, significantly negative enthalpy dominates the Gibbs free energy as little entropic changes would occur below 700°C, ensuring that the Al-substituted hollandite with higher Cs content is also more energetically stable.[4,37] The increased energetic stability with higher Cs content could be explained as follows. First, increasing Cs content decreases the distortion of octahedral framework to preserve the maximum symmetry of the hollandite.[36,38] Moreover, the amount of Al dopants on the B-sites is reduced in the higher Cs-containing hollandite to maintain charge neutrality. The synergistic effect of increased Cs content and reduction of Al dopants enhances the capacity for disorder in the octahedral framework and subsequently stabilizes the hollandite phase.[6] In addition, the strongly basic character of Cs_2O also makes hollandite formation exothermic with relatively acidic oxides.[6]

3.2.2 | Calculated enthalpies of formation

Calculated $\Delta H_{f,el}$ values from the sublattice model are listed in Table 5. Minor deviations of computed compositions

TABLE 2 Enthalpies of drop solution (ΔH_{ds}) in $3Na_2O{\cdot}4MoO_3$ solvent at 702°C and enthalpies of formation from constituent oxides ($\Delta H_{f,ox}$) and from the elements ($\Delta H_{f,el}$) of the hollandite compositions at 25°C. (Uncertainty is two standard deviations of the mean and the value in parentheses is the number of experiments.)

Sample	ΔH_{ds} (kJ/mol)	$\Delta H_{f,ox}$ (kJ/mol)	$\Delta H_{f,el}$ (kJ/mol)	ΔH_{rxn} (kJ/mol)
H1	364.1 ± 3.6 (9)	−199.1 ± 8.0	−8196.9 ± 9.8	−33.4 ± 12.9
H2	394.2 ± 8.2 (8)	−200.6 ± 10.4	−8149.7 ± 11.7	10.2 ± 13.6
H3	420.0 ± 7.5 (8)	−207.4 ± 9.5	−8117.1 ± 10.8	52.1 ± 10.5
H4	444.3 ± 13.7 (8)	−233.2 ± 14.5	−8047.9 ± 15.4	131.1 ± 10.5
H5	452.6 ± 10.2 (9)	−237.9 ± 10.8	−7958.9 ± 12.0	186.1 ± 5.4

TABLE 3 Enthalpies of drop solution in $3Na_2O{\cdot}4MoO_3$ solvent at 702°C (ΔH_{ds}) and enthalpies of formation from the elements ($\Delta H_{f,el}$) at 25°C of related binary constituent oxides. (Uncertainty is two standard deviations of the mean and the value in parentheses is the number of experiments.)

Oxide	ΔH_{ds} (kJ/mol)	$\Delta H_{f,el}$ (kJ/mol)
BaO	−184.61 ± 3.21[a]	−548.1 ± 2.1[d]
Cs_2O	−348.9 ± 1.7[b]	−346.0 ± 1.2[d]
α-Al_2O_3	96.6 ± 4.1 (6)	−1675.7 ± 1.3[d]
TiO_2	60.81 ± 0.11[c]	−944.0 ± 0.8[d]

[a] Ushakov et al.[30]

[b] Ushakov et al.[31]

[c] Putnam et al.[32]

[d] Robie and Hemingway.[33]

from measurements are a necessary compromise to acquire good agreement to both compositional data and $\Delta H_{f,ox}$ values. $\Delta H_{f,ox}$ values were calculated by subtracting the sum of the $\Delta H_{f,el}$ values of constituent oxides in Table 3 from the computed $\Delta H_{f,el}$ values in Table 5. It is notable that the $\Delta H_{f,el}$ value of each constituent oxide in Table 3 was multiplied by a coefficient prior to being summed. As indicated by Figure 2, the calculated $\Delta H_{f,ox}$ values using the sublattice model overall agree well with the experimental data in this work and prior DFT calculations.[36] More importantly, the general trend that the hollandite composition with higher Cs content possesses higher thermodynamic stability is reflected in Figure 2.

3.2.3 | Potential factors impacting thermodynamic stability

Size effects of framework cations and tunnel cations

The average ionic radius for A-site (R_A), B-site (R_B), and R_B/R_A was calculated and listed in Table S3 using the effective ionic radii reported by Shannon: Ba^{2+} = 1.42 Å and Cs^{+} = 1.74 Å in eightfold coordination, whereas Al^{3+} = 0.535 Å and Ti^{4+} = 0.605 Å in sixfold coordination.[39] As shown in Figure 3A, thermodynamic stability increases as R_B/R_A decreases agreeing with previous studies.[4,12,38]

Tolerance factor

Thermodynamic stability of hollandite structure can also be evaluated by tolerance factor t_H which is defined by the following expression:[4,12,40]

$$t_H = \frac{\left[(R_A + R_O)^2 - \frac{1}{2}(R_B + R_O)^2\right]^{\frac{1}{2}}}{\sqrt{\frac{3}{2}}(R_B + R_O)}, \quad (2)$$

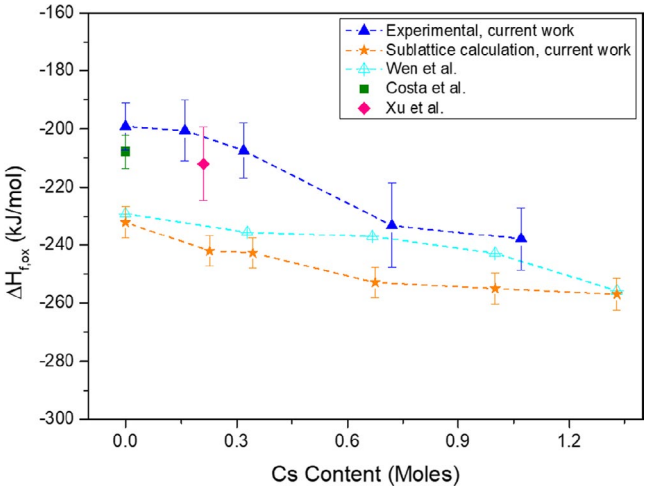

FIGURE 2 Experimentally derived and sublattice-based model calculated $\Delta H_{f,ox}$ for hollandite samples as a function of Cs content.[4,5,36] [Color figure can be viewed at wileyonlinelibrary.com]

TABLE 4 Thermochemical cycles used for calculation of the enthalpy of formation of H4 from constituent oxides ($\Delta H_{f,ox}$) and from the elements ($\Delta H_{f,el}$) at 25°C

Enthalpy of formation of H4 from its constituent oxides at 25°C ($\Delta H_{f,ox}$)	
$Ba_{0.67}Cs_{0.72}Al_{1.98}Ti_6O_{16}$ (s,25°C) → 0.67 BaO (sln,702°C) + 0.36 Cs_2O (sln,702°C) + 0.99 α-Al_2O_3 (sln,702°C) + 6 TiO_2 (sln,702°C)	ΔH_{ds}
0.67 BaO (s,25°C)→0.67 BaO (sln,702°C)	ΔH_1
0.36 Cs_2O (s,25°C)→0.36 Cs_2O (sln,702°C)	ΔH_2
0.99 α-Al_2O_3 (s,25°C)→0.99 α-Al_2O_3 (sln,702°C)	ΔH_3
6 TiO_2 (s,25°C)→6 TiO_2 (sln,702°C)	ΔH_4
0.67 BaO (s,25°C) + 0.36 Cs_2O (s,25°C) + 0.99 α-Al_2O_3 (s,25°C) + 6 TiO_2 (s,25°C) → $Ba_{0.67}Cs_{0.72}Al_{1.98}Ti_6O_{16}$ (s,25°C)	$\Delta H_{f,ox}$
$\Delta H_{f,ox} = \sum \Delta H_i$ (i = 1-4) − ΔH_{ds}	
Enthalpy of formation of H4 from the elements at 25°C ($\Delta H_{f,el}$)	
0.67 BaO (s,25°C) + 0.36 Cs_2O (s,25°C) + 0.99 α-Al_2O_3 (s,25°C) + 6 TiO_2 (s,25°C) → $Ba_{0.67}Cs_{0.72}Al_{1.98}Ti_6O_{16}$ (s,25°C)	$\Delta H_{f,ox}$
0.67 Ba (s,25°C) + 0.335 O_2 (g,25°C) → 0.67 BaO (s,702°C)	ΔH_5
0.72 Cs (s,25°C) + 0.18 O_2 (g,25°C) → 0.36 Cs_2O (s,702°C)	ΔH_6
1.98 Al (s,25°C) + 1.485 O_2 (g,25°C) → 0.99 α-Al_2O_3 (s,702°C)	ΔH_7
6 Ti (s,25°C) + 6 O_2 (g,25°C) → 6 TiO_2 (s,702°C)	ΔH_8
0.67 Ba (s,25°C) + 0.72 Cs (s,25°C) + 1.98 Al (s,25°C) + 6 Ti (s,25°C) + 8 O_2 (g,25°C) → $Ba_{0.67}Cs_{0.72}Al_{1.98}Ti_6O_{16}$ (s,25°C)	$\Delta H_{f,el}$
$\Delta H_{f,el} = \Delta H_{f,ox} + \sum \Delta H_i$ (i = 5-8)	

where R_A (R_B) is the average ionic radii of A-site (B-site) cations and R_O is the oxygen ion radii.[11,40] t_H values were reported in Table S3. In general, the thermodynamic stability of Al-substituted hollandite increases as t_H increases, which agree with the results of Fe-substituted hollandite reported by Zhao et al.[12]

Optical basicity

Thermodynamic stability such as enthalpy of formation can be affected by optical basicity as well.[4,12,41,42] If the stoichiometry of mixed oxides is known, theoretical optical basicity of mixed oxides or of any oxygen-containing solid can be calculated using the optical basicity of cations (Λ_{th}) in their appropriate coordination and valence.[43] Thus, the expression of optical basicity (Λ_H) of Al-substituted hollandite $Ba_{1.33-x}Cs_xAl_{2.66-x}Ti_{5.33+x}O_{16}$ can be developed as follows:

$$\Lambda_H = \frac{2\cdot(1.33-x)\Lambda_{Ba} + x\Lambda_{Cs} + 3\cdot(2.66-x)\Lambda_{Al} + 4\cdot(5.33+x)\Lambda_{Ti}}{32}. \quad (3)$$

Λ_{th} values were reported by Leboutiller and Courtine: Ba^{2+} = 1.25 and Cs^{+} = 1.70 in eightfold coordination, whereas Al^{3+} = 0.60 and Ti^{4+} = 0.75 in sixfold coordination.[42] Consequently, Λ_H values are given in Table S3. As expected in Figure 3C, thermodynamic stability is increased as increasing Λ_H.

3.3 | Implications for radionuclide immobilization

The significantly exothermic enthalpies of formation for H1-H5 indicate that they are very stable relative to their binary constituent oxides. However, in waste form applications, the hollandite phase is typically designed as one component of a multiphase system. In order to evaluate the suitability of Al-substituted hollandite as a waste form, stability must also be considered with respect to other potential phase assemblages which contain ternary oxides.[4,5] A phase assemblage containing $BaTiO_3$ perovskite is likely to form in synthetic rock (Synroc) systems, so the issue of stability can be addressed directly by thermodynamics. Equations 4 and 5 were used to demonstrate a widely utilized method for using the enthalpies of reaction (ΔH_{rxn}) at standard conditions to assess phase stability.[4-7,12]

$$Ba_{0.34}Cs_{1.07}Al_{1.64}Ti_{6.63}O_{16} = 0.34BaTiO_3 + 0.535Cs_2O + 0.82\alpha - Al_2O_3 + 6.29TiO_2 \quad (4)$$

$$\Delta H_{rxn,H5} = 0.34\Delta H_{f,ox(BaTiO3)} - \Delta H_{f,ox\ (H5)} = 186.1 \pm 5.4\ \text{kJ/mol} \quad (5)$$

where $\Delta H_{f,ox\ (H5)}$ was given in Table 2 and $\Delta H_{f,ox\ (BaTiO3)} = -152.3 \pm 4.0$ kJ/mol.[44] Thus, ΔH_{rxn} values of H1-H5 can be calculated and listed in Table 2.

Al_2TiO_5 was not considered as a decomposing phase due to its poor stability at ambient conditions.[5] Moreover, Cs–Al–O, Cs–Ti–O, Ba–Al–O, and Cs–Al–Ti–O phases are also possible to form, but they have not been reported in Synroc systems at ambient atmosphere. In addition, enthalpies of formation are not available for many of these phases.[5] Therefore, they were neglected in the above-mentioned phase stability analysis.[5,6]

As shown in Figure 4, it can be concluded that H2-H5 are energetically stable at room temperature with respect to $BaTiO_3$ perovskite, Cs_2O, α-Al_2O_3, and TiO_2 because of their endothermic ΔH_{rxn}. However, H1 is prone to decompose as determined by the exothermic ΔH_{rxn}. These analyses further convince the trend that more Cs content stabilizes the Al-substituted hollandite itself, which has been observed in Ga-, Zn- and Fe-substituted hollandites.[6,7,12] In addition, the relatively low Cs-containing samples are more likely to decompose and form soluble Cs-containing phases, which would further affect chemical durability of Al-substituted hollandite in aqueous solution.

3.4 | Chemical durability

3.4.1 | Aqueous leach testing

The fraction release of Cs, Ba, and Al from the hollandite samples are summarized in Figure 5. Fraction release was

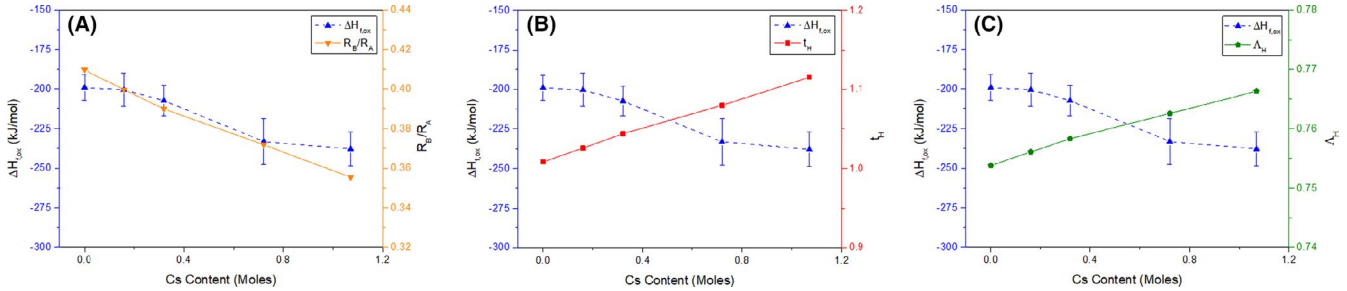

FIGURE 3 Variations of $\Delta H_{f,ox}$ and (A) R_B/R_A, (B) t_H, (C) Λ_H as a function of Cs content [Color figure can be viewed at wileyonlinelibrary.com]

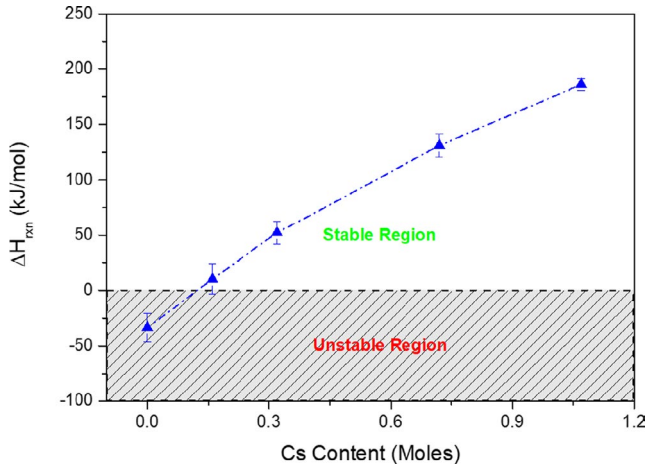

FIGURE 4 Variations of ΔH_{rxn} as a function of Cs content [Color figure can be viewed at wileyonlinelibrary.com]

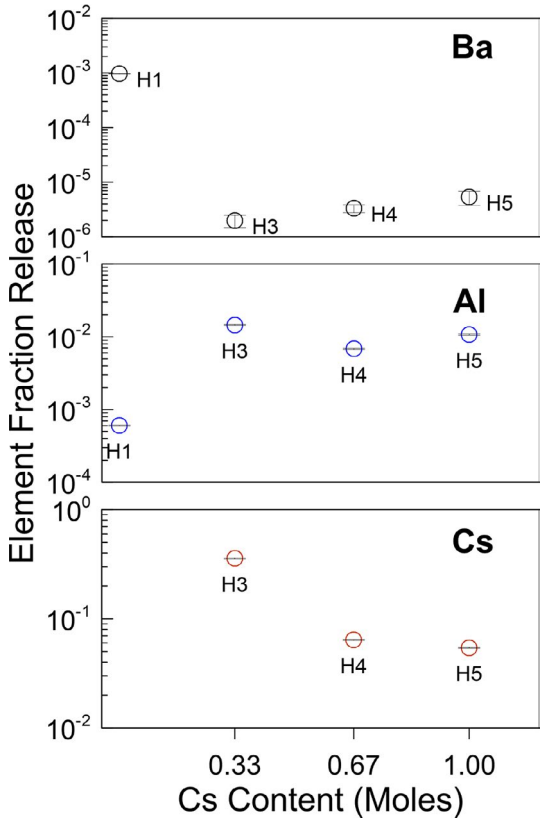

FIGURE 5 The fraction release of Cs, Ba, and Al from the hollandite samples as a function of Cs content [Color figure can be viewed at wileyonlinelibrary.com]

calculated as the fraction of the measured composition prior to leach experiments. The reported leach data are the gross total element fraction release and is not normalized to the surface area. Instead, steps were taken during the preparation to ensure the sample surface area to leachate volume was consistent. Less than one order of magnitude difference in surface area across all samples is a reasonable estimate and would be consistent with measured values for similar systems.[12] The measured fractional Cs release was five to seven times less in the H4 and H5 samples compared to that of the H3 sample, which supports the calorimetry measurements indicating that thermodynamic and phase stability (ie, $H_{f,ox}$ and H_{rxn}) of the Al-hollandite increases with increasing Cs content. Moreover, increasing Cs content appears to form particles that are increasingly physiochemically durable under the leach conditions tested. This phenomenon can be observed in representative SEM images of the particles taken before and after leaching and shown in Figure 6 and Figure S1. In Figure 6 and Figure S1, it is apparent that the particles were uniform in size before leaching but broke apart into smaller particles after leaching. In general, the number of the newly formed smaller particles decreased with increasing Cs content. In Figure 6, the interfaces between hollandite grains appear more discrete postleaching than preleaching. The magnitude of this effect increases with decreasing Cs content as evidenced by the visual difference among particles before and after leaching in the H3 sample, which diminishes in the H5 sample. The behavior is reminiscent of leaching of an intergranular phase and may be attributed to the formation of less-soluble Cs-containing phases in samples with less Cs content (eg, the H3 sample). Collectively, this analysis suggests an enhanced structural stability may accompany the Al-hollandite phase with increasing Cs content.

The dynamic surface area behavior observed during the leach testing is nontrivial to quantify and can complicate interpretation of the element release results. Indeed, the intent of following the PCT protocol was to ensure consistent samples were prepared to control the particle size and corresponding surface area. On the one hand, the observed trends in Cs release with Cs content in hollandite could be attributed to a corresponding difference in surface area, but the difference in surface areas, based on similarly prepared and previously measured for the analogous Fe-substituted hollandite series,[12] indicates the magnitude of a similar effect would be insufficient on its own to explain this data. Another possible explanation could be the prevalence of nondurable Cs-containing phases, for which the propensity to form alongside hollandite would increase with decreasing thermodynamic stability. In order to better understand the underlying mechanisms and elucidate the Cs release behavior, elution studies were performed on the hollandite samples prepared with the SCS methodology and doped with radioactive ^{137}Cs. Specifically, the H4 and H5 samples were selected because their physicochemical behavior during the leaching tests was more similar compared to the H3 sample.

3.5 | Elution studies of ^{137}Cs-doped hollandite

Elution studies of ^{137}Cs-doped samples were performed on the H4 and H5 compositions that exhibited excellent thermodynamic stability and chemical durability. Figure 7 provides

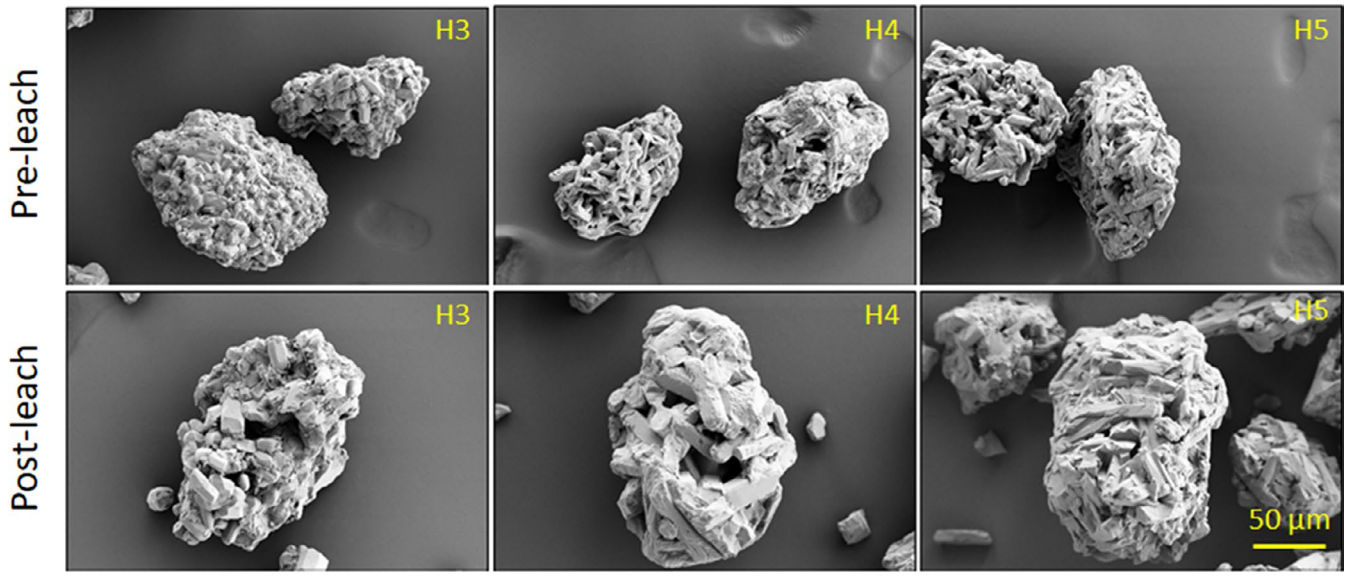

FIGURE 6 SEM images of the preleach (top) and postleach (bottom) hollandite particles, showing the evolution of the morphology as a function of Cs content [Color figure can be viewed at wileyonlinelibrary.com]

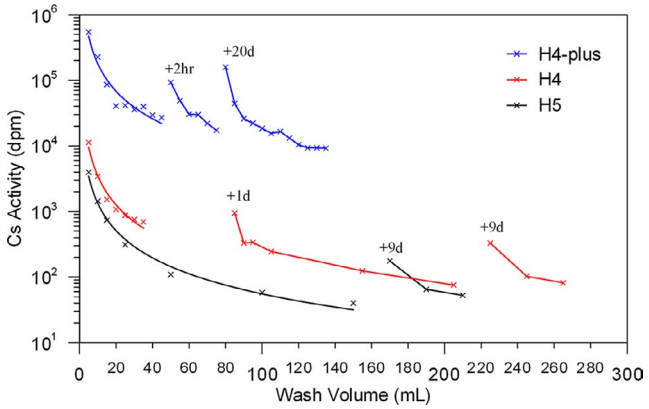

FIGURE 7 ^{137}Cs activity measured in eluate as a function of cumulative wash volume. Power fits to the data are overplayed for the 1st wash set of each sample. Relatively long time delays between data points are labeled; d = day, hr = hour [Color figure can be viewed at wileyonlinelibrary.com]

a plot of the activity of ^{137}Cs measured in the various washes from the initial count and after radiological equilibrium was reached for the three samples H4 and H5 were prepared with 0.4 µCi (1.5E4 Bq) and 0.2 µCi (7.5E3 Bq) of ^{137}Cs, respectively. H4-plus was prepared with 18µ Ci (1E6 Bq) of Cs, approximately two orders of magnitude greater activity. For each sample, two to three wash sets, separated by time, were conducted. The ^{137}Cs activity as a function of wash volume exhibited similar behavior for all samples, which appeared to follow a power-law relationship, consistent with a chemical desorption process. The amount of ^{137}Cs eluted continued to decrease with successive washes until the column was dried and the washing began again. When washing commenced after a time delay (eg, work interruption or start of a new wash set) an increase in ^{137}Cs was measured in the eluate, relative to the previous, but never reaching the initial wash concentration. This hysteresis-type behavior was reproducible and is indicated in Figure 7 by discontinuities in the data.

The significant majority, between 50% and 60%, of ^{137}Cs was eluted with the first 5 mL of wash water for a wash set. Greater than 90% of the total eluted ^{137}Cs occurred within the first 15 or 30 mL of wash water for the H5 and H4 compositions, respectively. In order to compare the ^{137}Cs release as a function of hollandite composition, the fraction of ^{137}Cs loss for each sample is presented for the first two washes and as a cumulative percentage over all wash sets in Table 6 and Figure 8, respectively. The results indicate that the H5 composition, which has more Cs content than the H4 compositions, released three to six times less ^{137}Cs compared to the H4 compositions in the first 10 mL of washing. Figure 8 shows the longer term behavior, which is comparable and confirmed less ^{137}Cs loss from the H5 composition than the H4 composition. Figure 8 also visually shows the more rapid approach to elution equilibrium for the H5 composition compared to the H4 composition—recall > 90% of the ^{137}Cs loss occurred within the first 15 mL for the H5 sample, compared to 30 mL for either H4 sample—which could be indicative of a higher order power function for the H5 composition. Taken together, these results support the premise that increased Cs concentration in hollandite suppresses total Cs loss.

Because ^{137}Cs will transmute into Ba during its decay, the retention of Ba and Cs in a hollandite structure as the material ages is of technical and scientific value. Therefore, a measure of the correlation between Ba and Cs release was conducted using sample H4-plus, which was the only sample with sufficient ^{137}Cs concentration

TABLE 5 Enthalpies of formation from constituent oxides ($\Delta H_{f,ox}$) and from the elements ($\Delta H_{f,el}$) for Al-substituted hollandite calculated from the thermodynamic database

Calculated Composition	$\Delta H_{f,ox}$ (kJ/mol)	$\Delta H_{f,el}$ (kJ/mol)
$Ba_{1.22}Al_{2.44}Ti_{5.56}O_{16}$	−232.1 ± 5.4	−8193.8
$Ba_{1.02}Cs_{0.227}Al_{2.28}Ti_{5.72}O_{16}$	−242.1 ± 5.3	−8150.4
$Ba_{0.926}Cs_{0.345}Al_{2.20}Ti_{5.80}O_{16}$	−247.8 ± 5.2	−8128.5
$Ba_{0.652}Cs_{0.675}Al_{1.98}Ti_{6.02}O_{16}$	−253.0 ± 5.2	−8068.9
$Ba_{0.330}Cs_{1.0}Al_{1.66}Ti_{6.34}O_{16}$	−255.0 ± 5.3	−7984.7
$Cs_{1.33}Al_{1.33}Ti_{6.67}O_{16}$	−257.0 ± 5.5	−7897.9

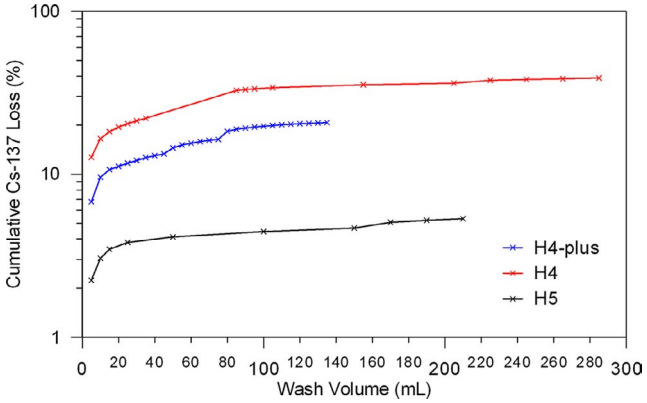

FIGURE 8 Cumulative ^{137}Cs loss combined for all wash sets [Color figure can be viewed at wileyonlinelibrary.com]

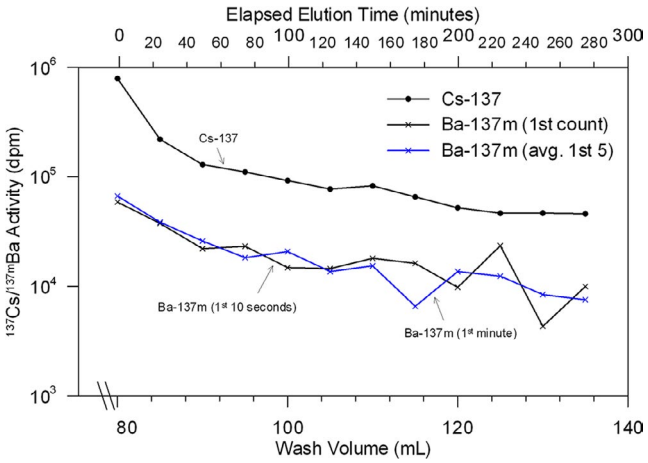

FIGURE 9 Comparison of ^{137m}Ba activity pre and postradiological equilibrium. Preradiological equilibrium is plotted after ~10 s (1st count) and ~1 min (average of first 5 counts). Postradiological equilibrium is equivalent to and shown as ^{137}Cs. Elution studies performed on samples doped with ^{137}Cs provided further evidence that increasing the Cs/Ba ratio increases Cs retention in hollandite for the composition range studied. Furthermore, these studies indicated that ^{137}Cs preferentially elutes compared to its daughter Ba in hollandite [Color figure can be viewed at wileyonlinelibrary.com]

to enable ^{137m}Ba measurements. Figure 9 provides a plot of the activity of the ^{137m}Ba 662 keV gamma-ray from the 3rd set of washes from the initial count (preradiological equilibrium) and after radiological equilibrium was reached. The preradiological equilibrium activity was calculated from the first count and from the average of the first five counts of each wash, which corresponded to ~10 seconds and ~1 minute, respectively. The postradiological equilibrium activity was equivalent to and labeled as ^{137}Cs. Radioactive Cs eluting from the hollandite during these experiments exhibited an average of ~7 times that of radioactive barium elution. The initial ^{137m}Ba activity measured was lower than the equilibrium values measured, which indicates a preferential elution of ^{137}Cs compared to its daughter, ^{137m}Ba. The concentration of stable cesium in the 1st and 7th washes was measured to compare with that of the radioactive cesium concentration. For those two washes, a difference in stable cesium concentration of ~92% was measured with ICP-MS, which was comparable, and within uncertainty, to the radioactive cesium concentration measured by gamma spectrometry of ~90%. Stable barium concentration was below the detection limit of ICP-MS in the 7th wash sample, and therefore the direct comparison of barium concentrations across the two washes could not be made. Nevertheless, the results of these radiological and nonradiological cesium and barium analyses demonstrate that radioactive cesium preferentially elutes compared to its radioactive barium daughter.

TABLE 6 Comparison of ^{137}Cs activity in the first two washes for each sample

	^{137}Cs Activity (1st Wash)		^{137}Cs Activity (2nd Wash)		
Hollandite sample	In first eluate (dpm/mL)	As % of loaded in sample	in second eluate (dpm/mL)	As % of loaded in sample	Ratio (1st/2nd)
H4-plus	5.41E5	6.7%	2.26E5	2.8%	2.4
H4	1.13E4	13%	3.41E3	3.8%	3.3
H5	3.97E3	2.2%	1.44E3	0.8%	2.7

4 | CONCLUSION

A series of Al-substituted hollandite samples with varying Cs content were synthesized. Calorimetric measurements suggested that the composition with more Cs content exhibited higher thermodynamic stability, which agreed well with calculations from reoptimized sublattice model. Moreover, enthalpies of formation of the samples were impacted by various factors, such as R_B/R_A, tolerance factor, and optical basicity. Results of aqueous leach testing revealed that chemical durability was greatly improved for the higher Cs-containing compositions, benefiting from less likely formation of soluble Cs-containing phases. Elution studies performed on samples doped with ^{137}Cs provided further evidence that increasing the Cs/Ba ratio increases Cs retention in hollandite for the compositional range studied. Furthermore, these studies indicated that ^{137}Cs preferentially elutes in hollandite compared to the Ba daughter decay product.

ACKNOWLEDGMENTS

KB, JA, SM, and TB acknowledge support of the Center for Hierarchical Waste Form Materials, an Energy Frontier Research Center funded by the US Department of Energy, Office of Science, Basic Energy Sciences under Award No. DE-SC0016574.

ORCID

Mingyang Zhao https://orcid.org/0000-0002-0752-7791
Kalee M. Fenker https://orcid.org/0000-0002-1656-9707
Kyle Brinkman https://orcid.org/0000-0002-2219-1253

REFERENCES

1. Cheary RW. Caesium substitution in the titanate hollandites $Ba_xCs_y(Ti^{3+}_{y+2x}Ti^{4+}_{8-2x-y})O_{16}$ from 5 to 400 K. Acta Crystallogr B. 1991;47:325–33.
2. Ghosh A, Sharma A, Talukder G. Effects of cesium on cellular systems. Biol Trace Elem Res. 1993;38(2):165–203.
3. Xu H, Costa GC, Stanek CR, Navrotsky A. Structural behavior of $Ba_{1.24}Al_{2.48}Ti_{5.52}O_{16}$ hollandite at high temperature: An in situ neutron diffraction study. J Am Ceram Soc. 2015;98(1):255–62.
4. Costa GC, Xu H, Navrotsky A. Thermochemistry of barium hollandites. J Am Ceram Soc. 2013;96(5):1554–61.
5. Xu H, Wu L, Zhu J, Navrotsky A. Synthesis, characterization and thermochemistry of Cs-, Rb- and Sr-substituted barium aluminium titanate hollandites. J Nucl Mater. 2015;459:70–6.
6. Zhao M, Xu Y, Shuller-Nickles L, Amoroso J, Frenkel AI, Li Y, et al. Compositional control of radionuclide retention in hollandite-based ceramic waste forms for Cs-immobilization. J Am Ceram Soc. 2019;102(7):4314–24.
7. Grote R, Zhao M, Shuller-Nickles L, Amoroso J, Gong W, Lilova K, et al. Compositional control of tunnel features in hollandite-based ceramics: structure and stability of (Ba, $Cs_{)1.3}3$(Zn, $T_{i)8O}16$. J Mater Sci. 2019;54(2):1112–25.
8. Carter M, Vance E, Mitchell D, Hanna J, Zhang Z, Loi E. Fabrication, characterization, and leach testing of hollandite, (Ba, Cs)(Al, $T_{i)2T}i_{6O}16$. J Mater Res. 2002;17(10):2578–89.
9. Cheary RW. The immobilisation of cesium in synroc. Mater Sci Forum. 1988;27(28):2578–89.
10. Carter M, Vance E, Li H. Hollandite-rich ceramic melts for the immobilisation of Cs. MRS Proc. 2003;807(249):1–6. https://doi.org/10.1557/PROC-807-249
11. Aubin-Chevaldonnet V, Caurant D, Dannoux A, Gourier D, Charpentier T, Mazerolles L, et al. Preparation and characterization of (Ba, Cs)(M, $T_i)_{8O}16$ (M = $^{Al}3+$, $^{Fe}3+$, $^{Ga}3+$, $^{Cr}3+$, $^{Sc}3+$, $^{Mg}2+$) hollandite ceramics developed for radioactive cesium immobilization. J Nucl Mater. 2007;366(1–2):137–60.
12. Zhao M, Russell P, Amoroso J, Misture S, Utlak S, Besmann T, et al. Exploring the links between crystal chemistry, cesium retention, thermochemistry and chemical durability in single-phase (Ba, $Cs_{)1.3}3$(Fe, $T_i)_{8O}16$ hollandite. J Mater Sci. 2020;55(15):6401–16.
13. Leinekugel-le-Cocq A, Deniard P, Jobic S, Cerny R, Bart F, Emerich H. Synthesis and characterization of hollandite-type material intended for the specific containment of radioactive cesium. J Solid State Chem. 2006;179(10):3196–208.
14. Cheary RW. An analysis of the structural characteristics of hollandite compounds. Acta Crystallogr B. 1986;42:229–36.
15. Leinekugel-le-Cocq-Errien A, Deniard P, Jobic S, Gautier E, Evain M, Aubin V, et al. Structural characterization of the hollandite host lattice for the confinement of radioactive cesium: quantification of the amorphous phase taking into account the incommensurate modulated character of the crystallized part. J Solid State Chem. 2007;180(1):322–30.
16. Pham D, Myhra S, Turner P. The surface reactivity of hollandite in aqueous solution. J Mater Res. 1994;9(12):3174–82.
17. Abdelouas A, Utsunomiya S, Suzuki T, Grambow B, Advocat T, Bart F, et al. Effects of ionizing radiation on the hollandite structure-type: $Ba_{0.85}Cs_{0.26}Al_{1.35}Fe_{0.77}Ti_{5.90}O_{16}$. Am Mineral. 2008;93(1):241–7.
18. Aubin V, Caurant D, Gourier D, Baffier N, Esnouf S, Advocat T. Radiation effects on hollandite ceramics developed for radioactive cesium immobilization. MRS Proc. 2003;792(R2.3):1–7. https://doi.org/10.1557/PROC-792-R2.3
19. Navrotsky A. Progress and new directions in high temperature calorimetry revisited. Phys Chem Miner. 1997;24(3):222–41.
20. Navrotsky A. Progress and new directions in calorimetry: a 2014 perspective. J Am Ceram Soc. 2014;97(11):3349–59.
21. Utlak SA, Besmann TM, Brinkman KS, Amoroso JW. Thermodynamic assessment of the hollandite high-level radioactive waste form. J Am Ceram Soc. 2019;102(10):6284–97.
22. Andersson JO, Guillermet AF, Hillert M, Jansson B, Sundman B. A compound-energy model of ordering in a phase with sites of different coordination numbers. Acta Metall Mater. 1986;34(3):437–45.
23. Havrig H. An extended version of the regular solution model for stoichiometric phases and ionic melts. Acta Chem Scand. 1971;25:3199–204.
24. Hillert M, Staffansson LI. Regular solution model for stoichiometric phases and ionic melts. Acta Chem Scand. 1970;24(10):3618–26.
25. Sundman B, Agren J. A regular solution model for phases with several components and sublattices, suitable for computer applications. J Phys Chem Solids. 1981;42(4):297–301.
26. Hillert M. The compound energy formalism. J Alloys Compd. 2001;320(2):161–76.
27. Hillert M. Some properties of the compound energy model. Calphad. 1996;20(3):333–41.
28. ASTM International C1285–14 standard test methods for determining chemical durability of nuclear, hazardous, and mixed waste glasses and multiphase glass ceramics: the

product consistency test (PCT). West Conshohocken, PA: ASTM International; 2014.
29. Xu Y, Wen Y, Grote R, Amoroso J, Nickles LS, Brinkman KS. A-site compositional effects in Ga-doped hollandite materials of the form $Ba_xCs_yGa_{2x+y}Ti_{8-2x-y}O_{16}$: implications for Cs immobilization in crystalline ceramic waste forms. Sci Rep. 2016;6:1–8.
30. Ushakov S, Cheng J, Navrotsky A, Wu J, Haile S. Formation enthalpies of tetravalent lanthanide perovskites by high temperature oxide melt solution calorimetry. MRS Proc. 2002;718(D7.17):1–6. https://doi.org/10.1557/PROC-718-D7.17
31. Ushakov SV, Navrotsky A, Farmer JM, Boatner LA. Thermochemistry of the alkali rare-earth double phosphates, $A_3RE(PO_4)_2$. J Mater Res. 2004;19(7):2165–75.
32. Putnam RL, Navrotsky A, Woodfield BF, Boerio-Goates J, Shapiro JL. Thermodynamics of formation for zirconolite ($CaZrTi_2O_7$) from T = 298.15 K to T = 1500 K. J Chem Thermodyn. 1999;31(2):229–43.
33. Robie RA, Hemingway BS. Thermodynamic properties of minerals and related substances at 298.15 K and 1 bar (105 Pascals) pressure and at higher temperatures. Washington: U.S. Government Printing Office; 1995.
34. Majzlan J, Navrotsky A, Casey WH. Surface enthalpy of boehmite. Clays Clay Miner. 2000;48:699–707.
35. Mazeina L, Navrotsky A. Surface enthalpy of goethite. Clays Clay Miner. 2005;53:113–22.
36. Wen Y, Xu Y, Brinkman KS, Shuller-Nickles L. Atomistic scale investigation of cation ordering and phase stability in Cs-substituted $Ba_{1.33}Zn_{1.33}Ti_{6.67}O_{16}$, $Ba_{1.33}Ga_{2.66}Ti_{5.67}O_{16}$ and $Ba_{1.33}Al_{2.66}Ti_{5.33}O_{16}$ hollandite. Sci Rep. 2018;8:1–11.
37. Wu L, Schliesser J, Woodfield BF, Xu H, Navrotsky A. Heat capacities, standard entropies and Gibbs energies of Sr-, Rb- and Cs-substituted barium aluminotitanate hollandites. J Chem Thermodyn. 2016;93:1–7.
38. Xu Y, Feygenson M, Page K, Nickles LS, Brinkman KS. Structural evolution in hollandite solid solutions across the A-site compositional range from $Ba_{1.33}Ga_{2.66}Ti_{5.34}O_{16}$ to $Cs_{1.33}Ga_{1.33}Ti_{6.67}O_{16}$. J Am Ceram Soc. 2016;99(12):4100–6.
39. Shannon RD. Revised effective ionic radii and systematic studies of interatomic distances in halides and chalcogenides. Acta Crystallogr A. 1976;32(5):751–67.
40. Kesson S, White T. Radius ratio tolerance factors and the stability of hollandites. J Solid State Chem. 1986;63(1):122–5.
41. Duffy JA. Ionic−covalent character of metal and nonmetal oxides. J Phys Chem A. 2006;110(49):13245–8.
42. Lebouteiller A, Courtine P. Improvement of a bulk optical basicity table for oxidic systems. J Solid State Chem. 1998;137(1):94–103.
43. Fierro JLG. Metal oxides: chemistry and applications, 1st edn. Boca Raton, FL: CRC Press; 2006.
44. Takayama-Muromachi E, Navrotsky A. Energetics of compounds ($A^{2+}B^{4+}O_3$) with the perovskite structure. J Solid State Chem. 1988;72(2):244–56.

SUPPORTING INFORMATION

Additional supporting information may be found online in the Supporting Information section.

How to cite this article: Zhao M, Amoroso JW, Fenker KM, et al. The effect of cesium content on the thermodynamic stability and chemical durability of $(Ba,Cs)_{1.33}(Al,Ti)_8O_{16}$ hollandite. *J Am Ceram Soc*. 2020;103:7310–7321. https://doi.org/10.1111/jace.17422